SUPPLEMENTARY INFORMATION

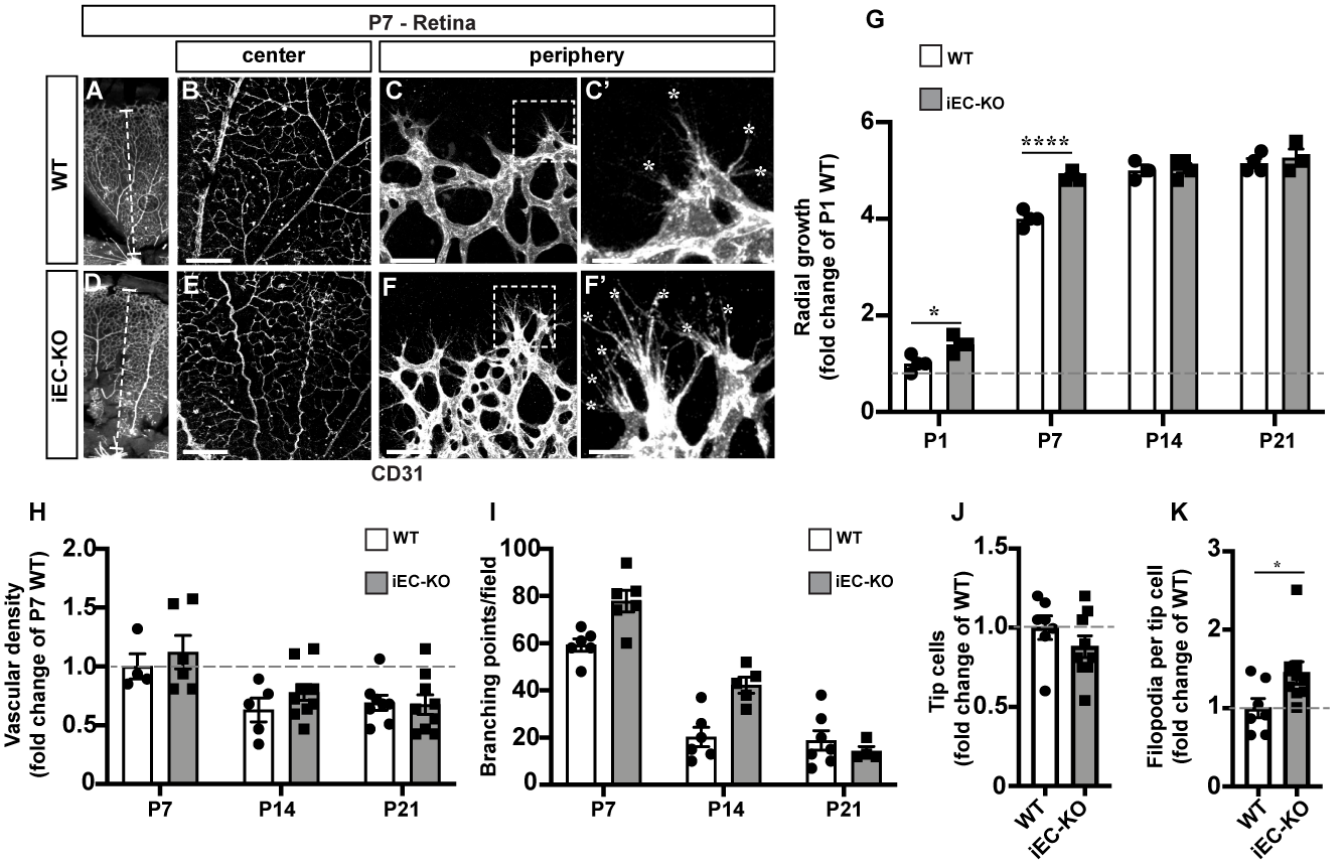

Figure S1 (related to Figure 2). Characterization of retinal vascular morphology in *Fgfbp1*$^{iEC\text{-}KO}$ mice during postnatal development.

(A-F') Immunofluorescence for CD31 (gray scale) in whole-mount retinas from wild-type (WT) (A, B, C, C') and *Fgfbp1*$^{iEC\text{-}KO}$ (D, E, F, F') P7 pups. Images in (B, E) were acquired at the center of the retina (scale bar: 200 µm). Images in C, F (scale bar: 100 µm) and their magnifications C' and F' (scale bar: 30 µm) were acquired in the periphery of the retina. Asterisks indicate filopodia in endothelial tip cells.

(G) Quantification of radial growth of the retinal vasculature in WT and *Fgfbp1*$^{iEC\text{-}KO}$ P1, P7, P14 and P21 pups. Each dot represents a single animal. There is a modest, but significant, increase in vessel radial growth in P1 and P7 mutant compared to wild-type pups. Data are presented as mean ± SEM; *: $p<0.05$, ****: $p<0.001$; Student's t-test (n = 3-4 mice / group).

(H) Quantification of retinal vascular density in WT and *Fgfbp1*$^{iEC\text{-}KO}$ P7, P14 and P21 pups. Each dot represents the average of at least three confocal acquisitions from a single animal. There are no differences between the two genotypes (Student's t-test). Data are presented as mean ± SEM (n = 4 - 8 mice/group).

(I) Quantification of the number of branching points of the retinal vasculature in WT and *Fgfbp1*$^{iEC\text{-}KO}$ at P7, P14 and P21. Each dot represents the average of at least three confocal acquisitions from a single animal. Data are presented as mean ± SEM (n = 4 - 8 mice / group). There are no differences between the two genotypes with the Student's t-test.

(J) Quantification of the number of tip cells and (K) filopodia per tip cell in the leading edge of the retinal vasculature in WT and *Fgfbp1*$^{iEC\text{-}KO}$ at P7, P14 and P21. Each dot represents the average of at least three confocal acquisitions from a single animal. Data are presented as mean ± SEM; *: $p<0.05$; Student's t-test (n = 6-8 mice / group).

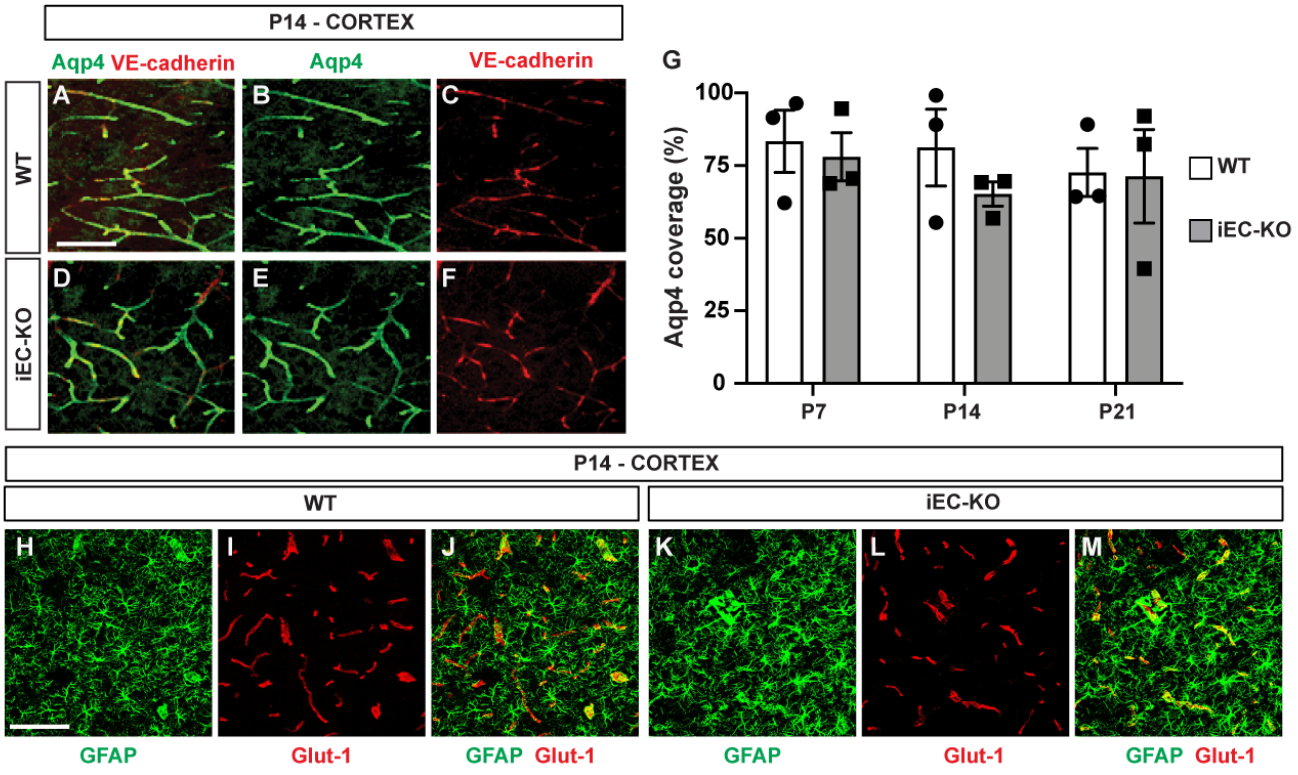

Figure S2 (related to Figure 3). Characterization of the astrocyte differentiation in *Fgfbp1*$^{iEC\text{-}KO}$ mice during postnatal cortical development.

(A-F) Analysis of the vascular coverage by astrocyte endfeet in the cortex of WT (A-C) and *Fgfbp1*$^{iEC\text{-}KO}$ (D-F) P14 pups. 100 µm thick brain sections were stained for Aquaporin4 (green, A, B, D and E) and VE-cadherin (red, A, C, D and F). Scale bar: 50 µm.

(G) Quantification of coverage of cortical vessels by the astrocytic endfeet in WT and *Fgfbp1*$^{iEC\text{-}KO}$ mice at P7, P14 and P21. Each dot represents the average of at least three confocal acquisitions from a single animal (n = 3 mice / group). There is no difference in coverage of the vasculature by the astrocyte endfeet in either genotype with the Student's t-test. Data are presented as mean ± SEM.

(H-M) Analysis of GFAP expression by astrocytes in the cortex of WT (H-J) and *Fgfbp1*$^{iEC\text{-}KO}$ (K-M) P14 pups. Sections were stained for GFAP (astrocyte marker; green, H, J, K, M) and Glut-1 (blood vessel marker; red, I, J, L, M). There is no difference in GFAP expression between two genotypes at P14. Scale bar: 100 µm.

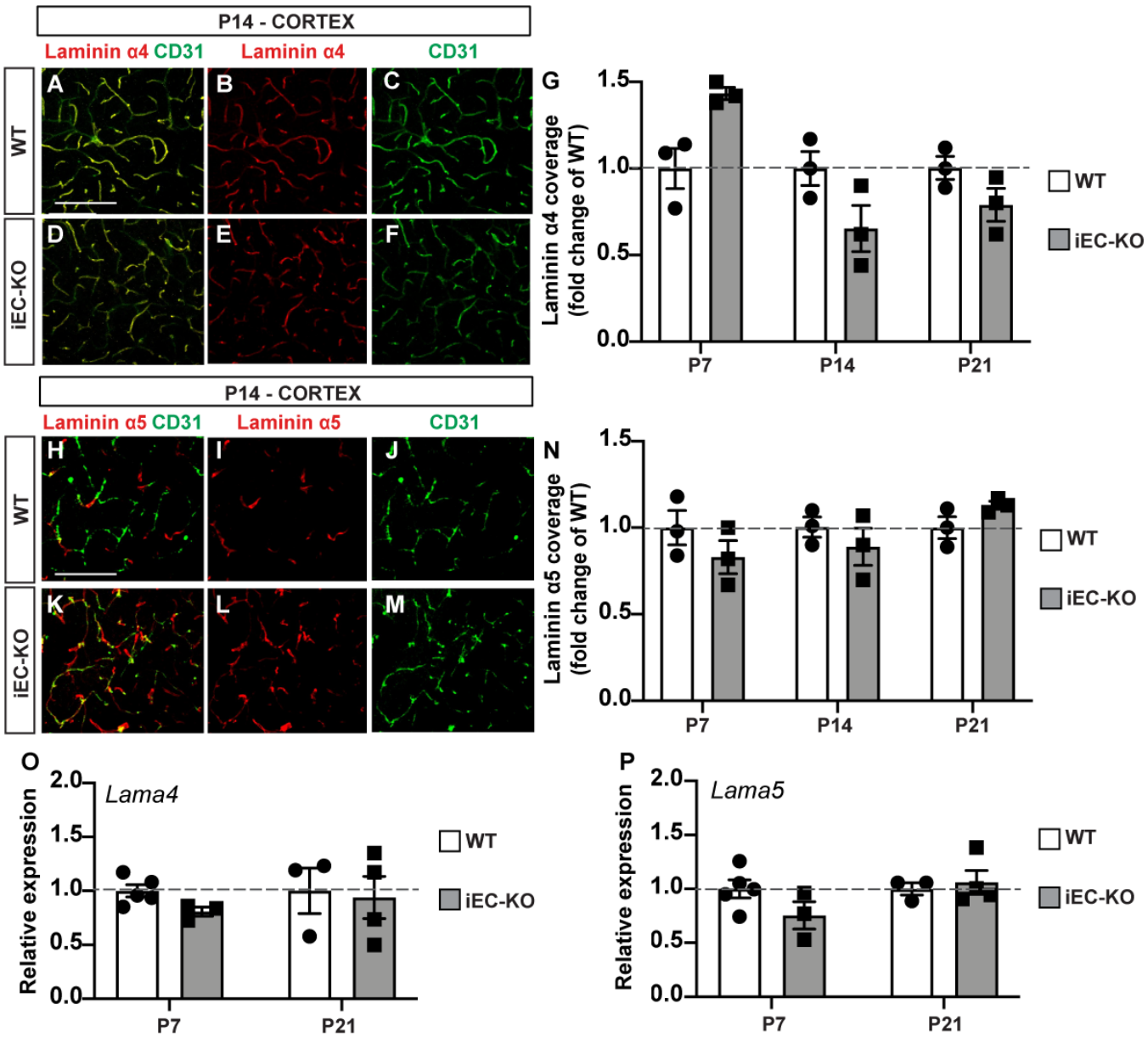

Figure S3 (related to Figure 5). Characterization of Laminin α4 and α5 deposition in the vascular basement membrane of *Fgfbp1*$^{iEC\text{-}KO}$ mice during postnatal cortical development.

(A-F) Analysis of Laminin α4 deposition in the vascular basement membrane of WT (A-C) and *Fgfbp1*$^{iEC\text{-}KO}$ (D-F) P14 cortexes. 100 µm thick brain sections were stained for CD31 (green; A, C, D, F) and Laminin α4 (red; A, B, D, E). Scale bar: 100 µm.

(G) Quantification of vessel coverage by Laminin α4 in the WT and *Fgfbp1*$^{iEC\text{-}KO}$ cortexes at P7, P14 and P21. Each dot represents the average of at least three confocal acquisitions from a single animal. There is no difference between the two genotypes (Student's t-test). Data are presented as mean ± SEM (n=3 mice / group).

(H-M) Analysis of Laminin α5 deposition in the vascular basement membrane of WT (H-J) and *FGFBP1*$^{iEC\text{-}KO}$ (K-M) P14 cortexes. 100 µm thick brain sections were stained for CD31 (green; H, J, K, M) and Laminin α5 (red; H, I, K, L). Scale bar: 100 µm.

(G) Quantification of vessel coverage by Laminin α5 in WT and *Fgfbp1*$^{iEC\text{-}KO}$ cortexes at P7, P14 and P21. Each dot represents the average of at least three confocal acquisitions from a single animal. There is no difference between the two genotypes (Student's t-test). Data are presented as mean ± SEM (n=3 mice / group).

(O-P) Dotted bar plots of the fold change in *Lama4* (O) and *Lama5* (P) mRNA expression within endothelial cells freshly isolated from brains of WT and *Fgfbp1*$^{iEC\text{-}KO}$ mice at P7 and P21. Each dot represents a single animal. Data are presented as mean ± SEM (n=3-5 mice / group). There is no difference between the two genotypes with the Student's t-test.

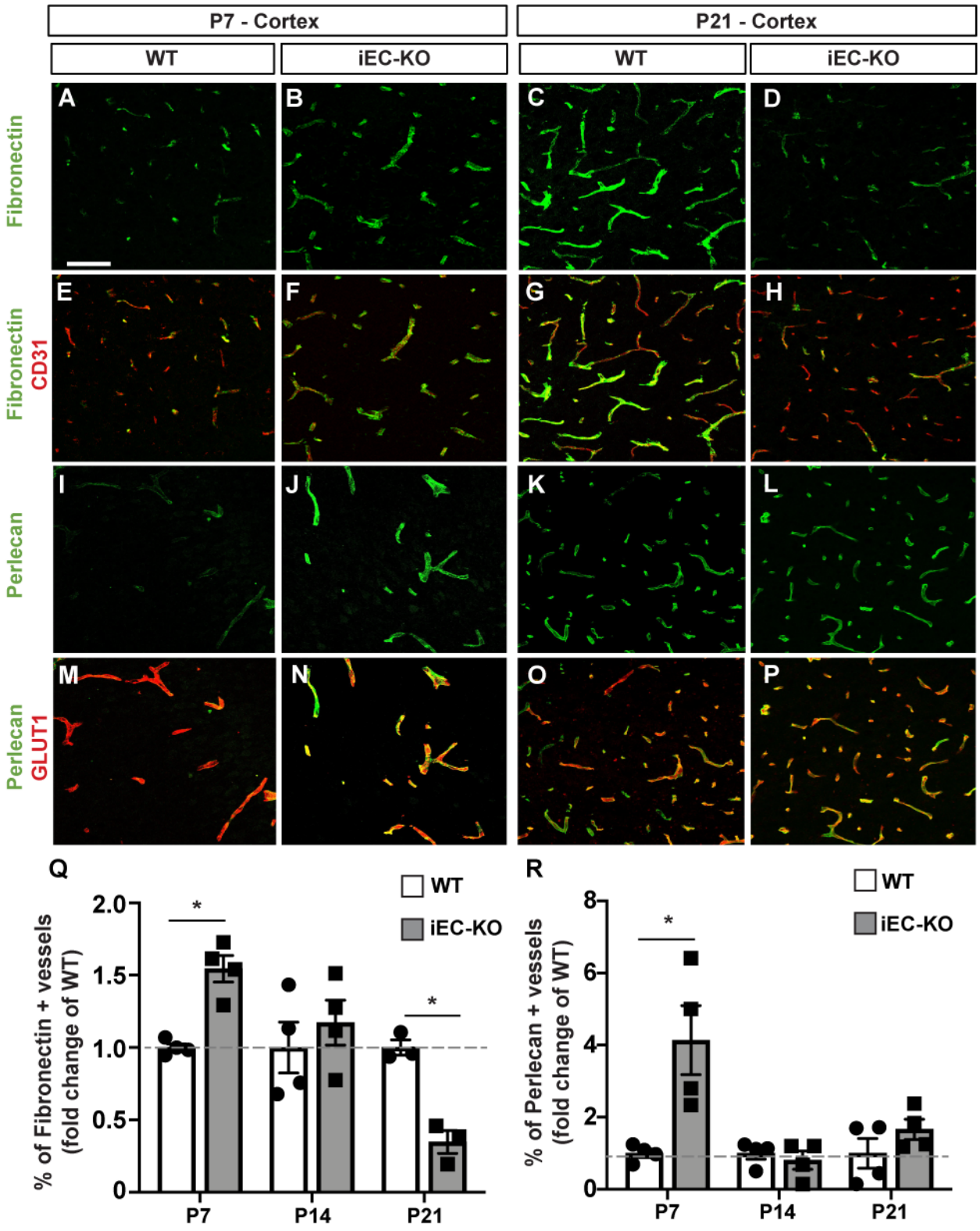

Figure S4 (related to Figure 5). Characterization of Fibronectin and Perlecan deposition in the vascular basement membrane of *Fgfbp1*$^{iEC\text{-}KO}$ mice during postnatal cortical development.

(A-H) Immunofluorescence analysis of Fibronectin deposition in the vascular basement membrane of WT (A, C, E, G) and *Fgfbp1*$^{iEC\text{-}KO}$ (B, D, F, H) cortexes at P7 (A, B, E, F) and P21 (C, D, G, H). Brain sections were stained for the vascular marker CD31 (red; E-H) and Fibronectin (green; A-H). Scale bar: 100 μm.

(I-P) Immunofluorescence analysis of Perlecan deposition in the vascular basement membrane of WT (I, M, K, O) and *Fgfbp1*$^{iEC\text{-}KO}$ (J, N, L, P) cortexes at P7 (I, J, M, N) and P21 (K, L, O, P). Sections were stained for the vascular marker Glut1 (red; M-P) and Perlecan (green; I-P). Scale bar: 100 μm.

(Q) Quantification of vessel coverage by Fibronectin in the cortex of WT and *Fgfbp1*$^{iEC\text{-}KO}$ mice at P7, P14 and P21. Each dot represents the average of at least six confocal acquisitions from a single animal (n = 4 mice /group). Data are presented as mean ± SEM. Fibronectin is increased in *Fgfbp1*$^{iEC\text{-}KO}$ animals at P7 and decreased at P21. *: $p<0.05$; Student's t-test.

(P) Quantification of vessel coverage by Perlecan in the cortex of WT and and *Fgfbp1*$^{iEC\text{-}KO}$ P7, P14 and P21 mice. Each dot represents the average of at least six confocal acquisitions from a single animal (n=4 mice / group). Data are presented as mean ± SEM. Perlecan is increased in *Fgfbp1*$^{iEC\text{-}KO}$ animals at P7; *: $p<0.05$; Student's t-test.

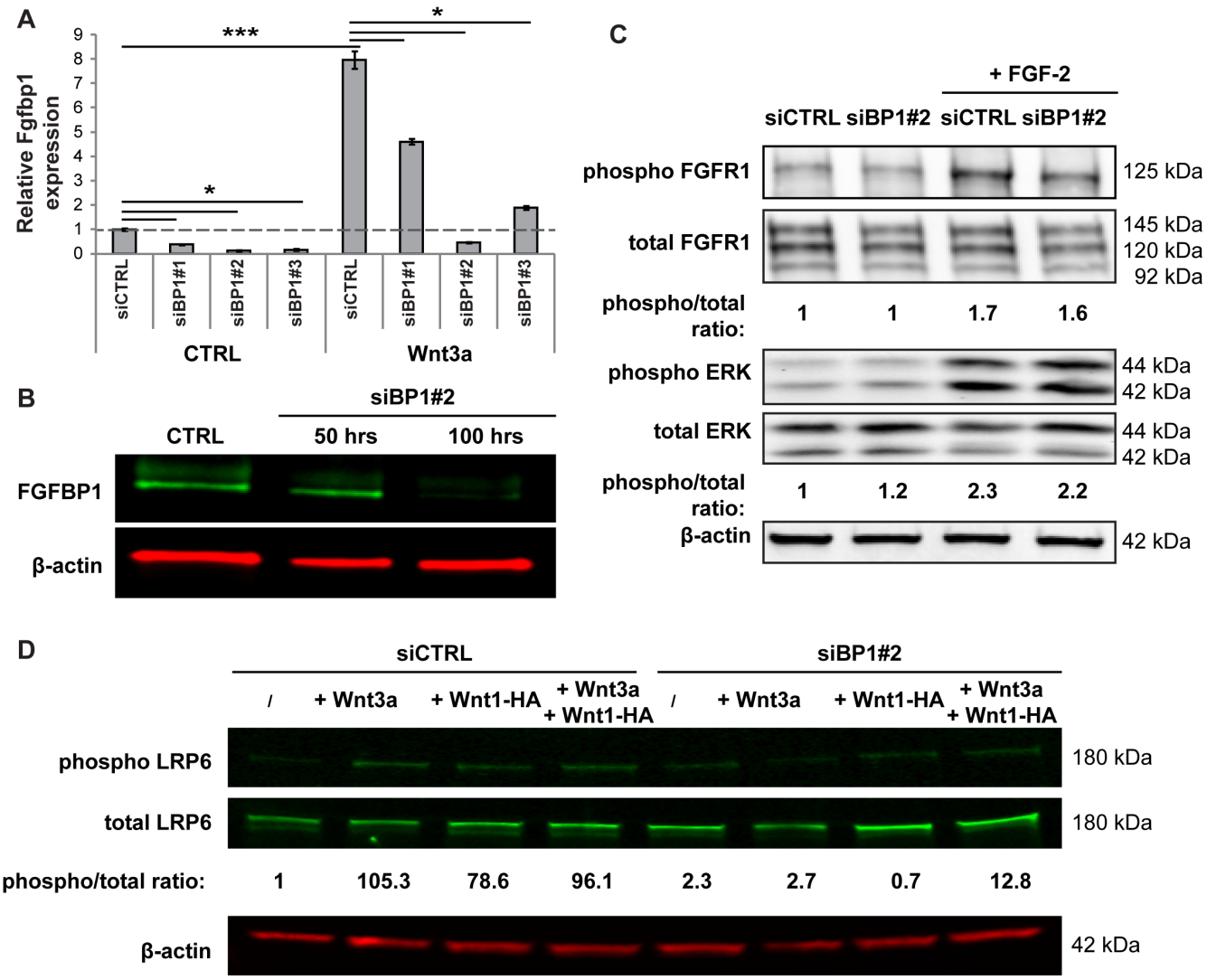

Figure S5 (related to Figure 6). Fgfbp1 is effectively downregulated by siBP1 *in vitro* and it is critical for phosphorylation of LRP6, but not FGFR1, receptor upon exposure to respective ligands.

(A) Fold change expression of *Fgfbp1* mRNA in untreated- versus Wnt-3a-treated-primary mouse brain endothelial cells (mBECs) transfected with either a scramble siRNA (siCTRL) or one of three different siRNAs targeting Fgfbp1 (siBP1#1, siBP1#2, siBP1#3). Data are presented as mean ± SD from three technical replicates (*: $p<0.05$, ***: $p<0.005$; one-way ANOVA).

(B) Western blot analysis of Fgfbp1 protein levels in mBECs transfected with either siCTRL or siBP1#2 for 50 or 100 hours after transfection. Fgfbp1 protein levels are downregulated significantly 100 hours after siBP1#2 transfection.

(C) Western blot analysis and quantification of the ratio of phosphorylated versus total FGFR1 and ERK levels in primary mBECs transfected with either siCTRL or siBP1#2, in the absence or presence of FGF-

2. The transfection with siBP1#2 does not affect FGF-2- induced phosphorylation of FGFR1 and ERK in primary mBECs.

(D) Western blot analysis and quantification of the ratio of phosphorylated versus total LRP6 levels in primary mBECs transfected with either siCTRL or siBP1#2 and treated with either Wnt3a, Wnt1-HA or sequential administration of both Wnt ligands. Different Wnt treatments induce LRP6 phosphorylation to comparable levels and this effect is abolished in siBP1#2-treated mBECs.

Table S1. Affymetrix analysis of genes that are either upregulated or downregulated in primary mBECs transfected with either siCTRL or siBP1#2 in the presence or absence of recombinant mouse Wnt3a. These genes were sorted either by a) percent change in expression levels in Wnt3a- versus control-treated primary mBECs that were tranfected with either siCTRL or siBP1#2. b) Wnt-regulated genes in siCTRL-transfected primary mBECs and c) Wnt-regulated genes in siBP1#2-transfected mBECs.

Click here to Download Table S1

Table S2. Genotyping protocols for mouse strains in this study

PCR assay	Target	Primers	Product sizes
LOXP1	Presence of 5' LoxP sequence	*LOXP1 Fw:* 5'-TCCACCCTGTTTCAAGTTGG *LOXP1 Rv:* 5'-GACCACCTGTTGGGAAAGG	*WT:* 210 bp *Tg:* 367 bp *Het:* 210 + 367 bp
LOXP2	Presence of 3' LoxP sequence	*LOXP2 Fw:* 5'-GAACACAGGCTTAAGGATACACC *LOXP2 Rv:* AGAGTACAGATCTACCACTGCTTCC	*WT:* 209 bp *Tg:* 357 bp *Het:* 209 + 357 bp
FGFBP1	Presence of recombined allele after tamoxifen injection	*LOXP1 Fw:* 5'-TCCACCCTGTTTCAAGTTGG *FGFBP1:* 5'-AATGCTTACCAGGTCTCTGTCC *CTRL Fw:* 5'-GGATTCAGCACGTTGGACC *CTRL Rv:* 5'-CTTCATAGGTGGCTGTCTGG	*WT:* no band *Tg:* 316 bp *CTRL:* 570 bp
VEC-CRE	Presence of Cdh5(PAC)-CreERT2 Tg	*CRE A:* 5'-CCAAAATTTGCCTGCATTACCGGTCGATGC *CRE B:* 5'-ATCCAGGTTACGGATATAGT *CTRL Fw:* 5'-GGATTCAGCACGTTGGACC *CTRL Rv:* 5'-CTTCATAGGTGGCTGTCTGG	*WT:* no band *Tg:* 1 kbp *CTRL:* 570 bp
R26-EYFP	Presence of Rosa26-EYFP transgene	*R26-4982:* 5'-AAGACCGCGAAGAGTTTGTC *R26-316:* 5'-GGAGCGGGAGAAATGGATATG *R26-883:* 5'-AAAGTCGCTCTGAGTTGTTAT	*WT*: 600 bp *Tg*: 320 bp *Het*: 320 + 600 bp

PCR assay	Target	Primers	Product sizes
Exon3/DEL	Identifies exon 3 deletion in β-cat$^{lox(ex3)/lox(ex3)}$ mice	*Exon3/DEL Fw:* GCTGCGTGGGACAATGGCTAC *Exon3/DEL Rv:* TGAGCCCTAGTCATTGCATAC	*WT*: 690 bp *Del*: 490 bp

Table S3. Fgfbp1 siRNA stealth sequences

	Name	Sequence
siFgfbp1#1	NM_008009_stealth_201	5’-CCTCGTTAGGGAAGGCCCAGAATAA
siFgfbp1#2	NM_008009_stealth_235	5’-CAGGACATCTAAATCTCTGACGCAT
siFgfbp1#3	NM_008009_stealth_406	5’-CGACAAAGACCAGATCTACTGGAAA

Table S4. TaqMan gene expression assays

Gene	Assay
Col4a1	Mm01210125_m1
Col4a2	Mm00802386_m1
Fgfbp1	Mm00456064_s1
Lama2	Mm00550083_m1
Lama4	Mm01193660_m1
Lama5	Mm01222029_m1
Plvap	Mm00453379_m1